Asymmetric quantum well broadband thyristor laser

Zhen Liu[1], Jiaqi Wang[1], Hongyan Yu[1], Xuliang Zhou[1], Weixi Chen[2], Zhaosong Li[1], Wei Wang[1], Ying Ding[3], Jiaoqing Pan[1]*

[1]Key Laboratory of Semiconductor Materials Science, Institute of Semiconductors, Chinese Academy of Science, College of Materials Science and Opto-Electronic Technology, University of Chinese Academy of Sciences, Beijing Key Laboratory of Low Dimensional Semiconductor Materials and Devices, Beijing 100083, China
[2]State Key Laboratory for Macroscopic Physics and School of Physics, Peking University, Beijing, 100871, China
[3]School of Engineering, University of Glasgow, Glasgow G12 8LT, UK
*Corresponding author: jqpan@semi.ac.cn

Z. Liu, and J. Wang contributed equally to this work.

Abstract: A broadband thyristor laser based on InGaAs/GaAs asymmetric quantum well (AQW) is fabricated by Metal Organic Chemical Vapor Deposition (MOCVD). The 3-μm-wide Fabry-Perot (FP) ridge-waveguide laser shows an S-shape I-V characteristic and exhibits a flat-topped broadband optical spectrum coverage of ~27 nm (Δ_{-10} dB) at a center wavelength of ~1090 nm with a total output power of 137 mW under pulsed operation. The AQW structure was carefully designed to establish multiple energy states within, in order to broaden the gain spectrum. An obvious blue shift emission, which is not generally acquired in QW laser diodes, is observed in the broadening process of the optical spectrum as the injection current increases. This blue shift spectrum broadening is considered to result from the prominent band-filling effect enhanced by the multiple energy states of the AQW structure, as well as the optical feedback effect contributed by the thyristor laser structure.

Key words: broadband laser; asymmetric quantum well; thyristor
EEACC: 4320J

1. Introduction

It is highly desirable for semiconductor optical sources to present broadband spectra characteristics for various applications, such as ultra-short pulse generation, spectroscopy imaging, and wavelength-division multiplexing-passive optical network (WDM-PON)[1-4]. Particularly, semiconductor broadband lasers are much preferable for their high output power, comparing with conventional semiconductor broadband sources such as superluminescent diodes (SLDs) and semiconductor optical amplifiers (SOAs). Various kinds of broadband semiconductor lasers have been reported, such as quantum cascade lasers (QCLs)[5], quantum dots (Qdots) lasers[6], quantum dash (Qdash) lasers[7], quantum well thyristor lasers[8, 9] etc.

The basicidea in these methods is to establish multiple quantized energy states in the gain media to broaden the gain spectrum. Efforts have been made to achieve broadband lasing spectra using an asymmetric quantum well (AQW)[10] as the active layer materials. By conveniently tuning the width of quantum wells or barriers of the AQW, multiple quantized energy states can be generated and the gain bandwidth can be broadened. However, there is still no reports on AQW lasers for broadband lasing spectrum generation to the best of our knowledge. Oh-Kee Kwon et al. [11] reported an AQW laser with complex multi-quantum wells but illustrated only a wide modal gain spectrum instead of a lasing spectrum. The main obstacle for an AQW laser to achieve a broad stimulated emission is the different pumping and lasing rate in the asymmetric quantum wells of different width.

In this letter, we proposed a broadband InGaAs/GaAs AQW laser with a thyristor-like structure emitting a broad lasing spectrum of 27 nm and a high output power of 137 mW. The possible dynamics of optical feedback effect and inner oscillation of the thyristor-like structure may help the achievement of lasing in AQWs. The spectrum broadens towards the blue direction as the injection current increases, and meanwhile gets flat-topped, which is beneficial to applications requiring a uniform distribution of optical power across a broad wavelength range. Compared with the QW thyristor lasers, the AQW thyristor laser has an advantage of achieving a broad spectrum at lower injection currents, because of the broad gain spectrum resulted from the multiple energy states in AQW structure.

2. Experiments

Table 1. The structure of the AQW broadband thyristor laser

Material	Thickness(nm)	Doping Concentration (cm^{-3})
GaAs	300	C-1×10^{20}
$Al_{0.47}Ga_{0.53}As$	1800	C-1×10^{18}
$Al_{0.47}Ga_{0.53}As$	35	Si -1×10^{19}
GaAs	10	Si -1×10^{19}
GaAs	8	
$Al_{0.47}Ga_{0.53}As$	35	
$Al_{0.26\text{-}0.47}Ga_{0.74\text{-}0.53}As$	55	
GaAs	80	
InGaAs	15	
GaAs	15	
InGaAs	5	
GaAs	400	
$Al_{0.26}Ga_{0.74}As$	100	
$Al_{0.47}Ga_{0.53}As$	1800	Si-1×10^{19}
GaAs buffer	400	Si-1×10^{19}

Table 1. shows the structure of the AQW broadband thyristor laser. It was grown on a heavily n-doped (0 0 1) exact-oriented GaAs substrate via MOCVD (Aixtron 3x2FT system) using only one step growth. The growth temperature was varied from 680 °C to 830 °C.

The structure consists of an AQW active region, an 80-nm and 400-nm asymmetric broad waveguide, a 1.8-μm $Al_{0.47}Ga_{0.53}As$ cladding layers, and a 300-nm p+-GaAs cap layer. Besides, by inserting a 35-nm n+-$Al_{0.47}Ga_{0.53}As$ layer and a n+-GaAs layer under p-$Al_{0.47}Ga_{0.53}As$ cladding, the whole structure can be considered as a PNiN thyristor. The AQW active region consists of a 5-nm and a 15-nm $In_{0.29}Ga_{0.71}As$ quantum well and is separated by a 15-nm GaAs barrier in order to acquire a broaden gain spectrum.

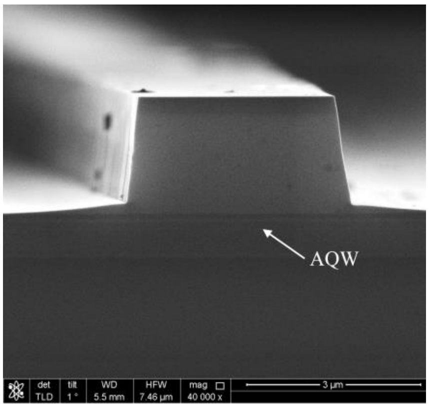

Fig. 1. Scanning electron microscope photograph of the ridge waveguide structure of the AQW laser.

A ridge waveguide with a width of 3 μm and a depth of 2.1 μm was fabricated by standard lithography and Inductively Coupled Plasma (ICP) dry-etching as shown in Fig. 1. A 150-nm silicon dioxide insulating layer was deposited by Plasma-Enhanced Chemical Vapor Deposition (PECVD), and a metal contact window was defined by self-aligned lithography technology. Then, the p-type contact metal Ti/Au was deposited by magnetron sputtering and n-type ohmic contact was deposited by the thermal evaporation of Au/Ge/Ni with 450 ºC, 30 s annealing in a Rapid Thermal Processor (RTP). Finally, the wafers were cleaved into 1000-μm bars and both of front and end facets were coated with TiO_2/Al_2O_3 multiple layers in order to obtain AR/HR mirror reflectivity of 14.7% and 97%, respectively. After coating on both facets of the laser bars, the lasers were separated into individual chips and mounted p-side up on the temperature-controlled indium coated copper heat sink under pulsed operation (5-μs pulse width and 0.5% duty cycle).

3. Results and discussion

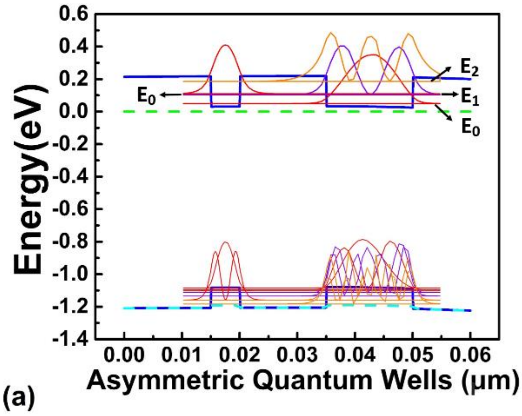

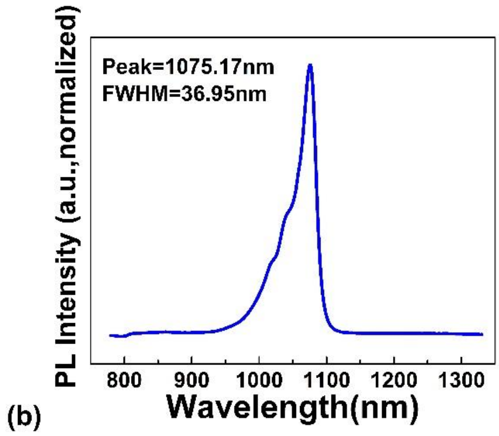

Fig. 2. (a) Calculated energy states of InGaAs/GaAs AQW at equilibrium simulated by commercial software Crosslight (Crosslight Software, Inc., Canada). (b) Room temperature PL spectrum of InGaAs/GaAs AQW.

Fig. 2(a). shows the calculated energy states and wave functions of InGaAs/GaAs AQW using a commercial simulation software Crosslight PIC3D (Crosslight Software, Inc., Canada). The quantized energy states in each well are denoted by E_0, E_1, and E_2 from the fundamental level in sequence. It is obvious that the E_0 energy state in the wider well is lower than that in the narrower well. Fig. 2(b). illustrates a broadening of the PL spectrum with the FWHM of 36.95 nm and peak wavelength at 1075.17 nm at room temperature. This results from a collective contribution of the multiple energy states in the InGaAs/GaAs AQW active region [12].

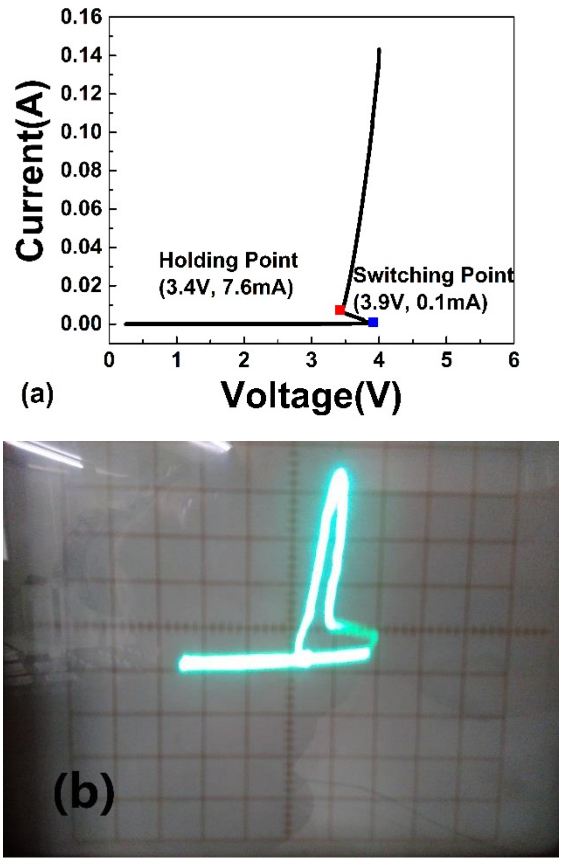

Fig. 3. (a) Nonlinear forward S-shape I-V characteristic of the AQW laser. (b) A similar measurement was taken with a homemade XJ4810 oscilloscope (curve tracer).

Fig. 3(a) shows the nonlinear S-shape I-V characteristic of an AQW laser measured by a precision source/measure unit (Agilent B2902A). It can be clearly observed from the I-V characteristics under forward bias that the nonlinear S-shape is composed of three zones including the low-current OFF state, the high-current ON state, and the negative differential resistance (NDR) region, for the device structure can be considered as a PNiN thyristor as a whole. The switching voltage and current are measured as 3.9 V and 0.1 mA, and the holding voltage and current are 3.4 V and 7.6 mA, respectively. A similar I-V curve and hysteresis are observed by a homemade XJ4810 oscilloscope (transistor curve tracer) in Fig. 3(b) under alternating current pumping.

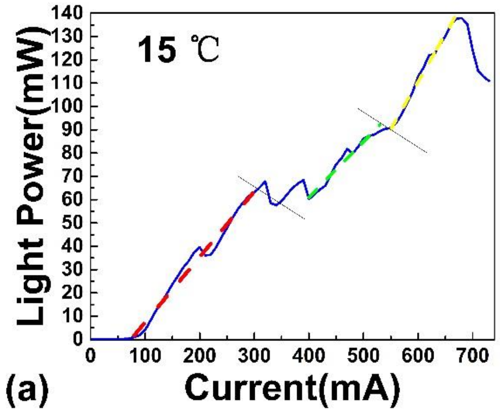

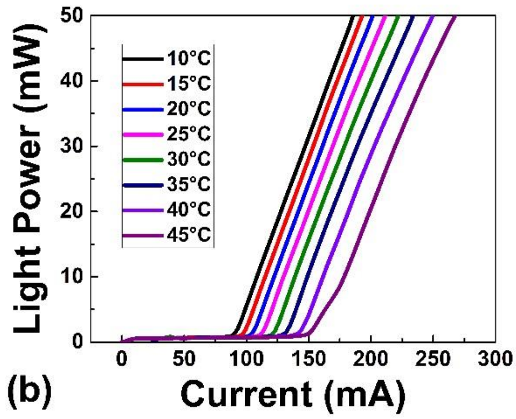

Fig. 4. (a) The L-I curve of the AQW laser testing at 15°C . (b) L-I curves tested near the threshold under varied temperatures from 10 °C to 45 °C .

An carrier optical feedback effect has been reported to be exist in the thyristor laser structure, which may improve the optical gain, differential gain, and temperature stability of our AQW thyristor laser[13, 14]. The output power versus injection current curve (L-I) of a representative laser is depicted in Fig. 4(a). The laser has a threshold current of 97.8 mA under 15°C, corresponding to a current density of 3.26 kA/cm^2. The maximum single facet output power of 137 mW is achieved at an injection current level of 670 mA.

Note that there are several kinks at ~300 mA and ~600 mA in the L-I curve. We separate the L-I curve into three operating ranges with different slope efficiencies, which corresponds to a varied gain characteristic caused by AQW. For simplicity, the three regions are colored red, green, and yellow as in Fig. 4(a), with the slope efficiency of 0.28 W/A, 0.23 W/A, and 0.40 W/A, respectively.

This interesting phenomenon can be mainly attributed to the lasing of the different energy states in each well. In the red region, a smooth L-I curve indicates the laser operating at the E_0 energy state in the wider well, while in the green region, the slope efficiency becomes lower for the restriction of gain saturation of the E_0 energy state. In addition, with the increase of injection current, it can be clearly noticed that the slope efficiency in the yellow region increases sharply, which is attributable to the simultaneous lasing of both the E_0 energy state in each well and E_1 energy state in the wider well.

By changing the testing temperature in the range of 10-45 °C, a set of light power versus current (L-I) curves near the threshold is depicted in Fig. 4(b). From the dependence of I_{th} on temperature, the characteristic temperature T_0 of 65 K has been obtained, which shows a better level compare to Qdots[6] and Qdash[7] broadband laser.

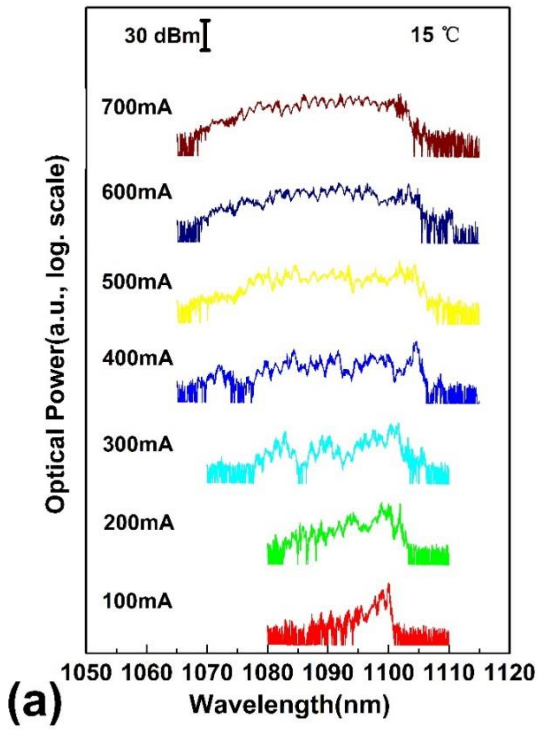

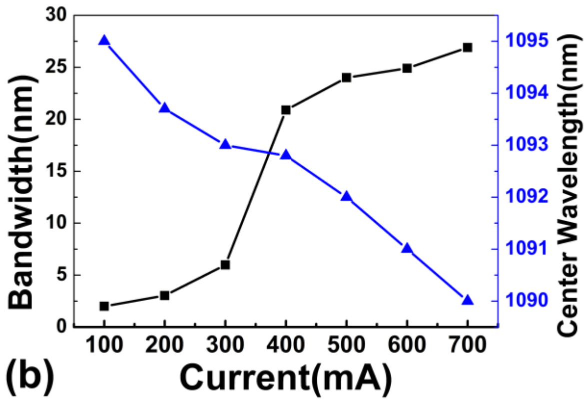

Fig. 5. (a) Lasing spectra in a logarithmic scale under various current levels from 100 mA to 700 mA at 25 °C. (b) The corresponding spectral bandwidth measured at Δ_{-10} dB levels and center wavelength as a function of current.

Fig. 5(a) shows laser spectra taken in different pulse currents from 100 mA to 700 mA at 15 °C, measured by an optical spectrum analyzer (ADVANTEST Q8384) with a resolution of 0.01 nm under high-sense mode. With an increased injection current, a progressive blue shift in the lasing spectra is noticed due to a prominent band-filling effect[10]. At a high injection level, the blue-shift and red-shift can be observed simultaneously. The red-shift of the wavelength results from the temperature effect and band gap shrinkage with increasing current of the active region[15,16]. The lasing spectrum reaches its largest bandwidth at 700 mA, with a Δ_{-10} dB bandwidth of 27 nm, corresponding to side-mode suppression ratio over 30 dB. The center wavelength of the spectrum goes from 1095 nm to 1090 nm as the current increases. It can also be seen that the spectral bandwidth and center wavelength are proportional to the injection current in Fig. 5(b).

The broadening of the spectrum toward the short wavelength and variation of center wavelength can be explained by the transition of carriers between energy states. Under low injection currents, the carriers fill the E_0 energy state in the wider well primarily, corresponding to the lasing spectrum centered at 1095 nm under a 100 mA injection current. As the injection level increases, carriers tend to transport to higher energy states of the E_0 energy state of the narrower well and the E_1 energy state of the wider well. Thus the spectrum broadens and becomes nearly flat-topped as the distribution of carriers varies, with a sharp increase in the slope efficiency as mentioned above. Meanwhile, the center of the spectrum moves toward a shorter wavelength. Besides, the flat-topped broad spectrum might have something to do with the dynamic process introduced by the special thyristor-like material structure, such as the optical feedback effect and possible inner oscillation produced by the NDR region on the I-V curve. Limited by the measuring equipment now available, the dynamic of the optic spectrum was not characterized in this paper, which would be further researched later on.

4. Conclusion

In summary, we have demonstrated a flat-topped broadband lasing emission using InGaAs/GaAs AQW laser at a center wavelength of ~1090 nm. The multiple energy states established in the AQW structure contributes to the broadening of spectrum towards the blue side. The laser exhibits a Δ_{-10} dB level broadband spectrum width of 27 nm along with a 137-mW output power. Our result is a step forward in achieving a broadband emission laser with a simpler and more controllable technique. By carefully optimizing the width and height of wells and barriers in AQW, the gain spectrum can be further broadened to improve the emission bandwidth of the AQW broadband laser. Our result leads to potential applications, such as mode locking with ultra-short pulse generation, biomedical imaging, broad wavelength tunability, and multi-wavelength generation.

This work was supported by the National Natural Science Foundation of China (NSFC) (61604144, 61504137).

Acknowledgement

The authors would like to thank Huolei Wang, Jing Bian, Lijun Yuan, Baojun Wang, and Junping Mi for their contributions to this paper.

References

[1] Shidlovski V R, Wei J. Superluminescent diodes for optical coherence tomography. Proc SPIE Test and Measurement Applications of Optoelectronic Devices, 2002, 4648: 139

[2] Maeda Y, Yamada M, Endo T, et al. 1700 nm ASE light source and its application to mid-infrared spectroscopy. Optoelectronics and Communication Conf and Australian Conf on Opt Fibre Technol, 2014

[3] Heo D, Lee J S, Yun I K, et al. Polarization-independent, high-power, and angle-flared superluminescent diode for WDM-PON applications. Proc IEEE LEOS Annual Meeting Conf, 2005

[4] Shin D J, Keh Y C, Kwon J W, et al. Low-cost WDM-PON with colorless bidirectional transceivers. J Lightwave Technol, 2006, 24(1): 158

[5] Gmachl C, Sivco D L, Colombelli R, et al. Ultra-broadband semiconductor laser. Nature, 2002, 415: 883

[6] Djie H S, Ooi B S , Fang X M, et al. Room-temperature broadband emission of an InGaAs/GaAs quantum dots laser. Opt Lett, 2007, 32: 44

[7] Djie H S, Tan C L, Ooi B S, et al. Ultrabroad stimulated emission from quantum-dash laser. Appl Phys Lett, 2007, 91: 111116

[8] Wang H, Zhou X, Yu H, et al. Ultrabroad stimulated emission from quantum well laser. Appl Phys Lett, 2014, 104: 251101

[9] Slipchenko S O, Podoskin A A, Rozhkov A V, et al. A study of nonlinear lasing dynamics of an InGaAs/AlGaAs/GaAs heterostructure power laser-thyristor emitting at 905nm. J Appl Phys, 2014, 116: 084503

[10] Lin C F, Lee B L, Lin P C. Broad-band superluminescent diodes fabricated on a substrate with asymmetric dual quantum wells. IEEE Photonics Technol Lett, 1996, 8: 1456

[11] Kwon O K, Kim K, Sim E D, et al. Asymmetric multiple-quantum-well laser diodes with wide and flat gain. Opt Lett, 2003, 28: 2189

[12] Khan M Z M, Ng T K, Lee C S, et al. Chirped InAs/InP quantum-dash laser with enhanced broad spectrum of stimulated emission. Appl Phys Lett, 2013, 102: 091102

[13] Podoskin A A, Soboleva O S, Zakharov M S, et al. Optical feedback in 905 nm power laser-thyristors based on AlGaAs/GaAs heterostructures. Semicond Sci Technol, 2015, 30: 125011

[14] Slipchenko S O, Podoskin A A, Rozhkov A V, et al. High-Power Laser Thyristors With High Injection Efficiency (λ = 890–910 nm). IEEE Photonics Technol Lett, 2015, 27: 307

[15] Bennett B R, Soref R A, Del Alamo J A. Carrier-Induced Change in Refractive Index of InP, GaAs, and InGaAsP. IEEE J Quantum Electron, 1990, 26: 113

[16] Chen P A, Chang C Y, Juang C. Carrier-Induced Energy Shift in GaAs/AlGaAs Multiple Quantum Well Laser Diodes. IEEE J Quantum Electron, 1993, 29: 2607

非对称量子阱宽谱晶闸管激光器

刘震[1]，王嘉琪[1]，于红艳[1]，周旭亮[1]，陈娓兮[2]，李召松[1]，王圩[1]，丁颖[3]，潘教青[1]

[1]中国科学院半导体研究所材料重点实验室, 中国科学院大学材料科学与光电技术学院, 低维半导体材料与器件北京市重点实验室，北京 100083；

[2]北京大学物理学院人工微结构和介观物理国家重点实验室, 北京 100871；

[3]格拉斯哥大学物理学院, 格拉斯哥 G12 8LT, 英国

摘要：本文报道了一种含 InGaAs/GaAs 非对称量子阱的宽谱晶闸管半导体激光器，为脊波导 F-P 腔结构，脊宽 3 μm。通过非对称量子阱的有源区设计，并利用一种晶闸管型材料结构，实现了脉冲工作下 Δ_{-10} dB 谱宽为 27 nm 的宽光谱激射，中心波长 1090 nm。其光谱随注入电流的增大向短波长方向显著展宽，这一现象与非对称阱中的能级填充效应相一致，并可与激光器中的光反馈等动态过程相关。通过进一步优化非对称量子阱，光谱宽度有望获得提高。该宽谱激光器有体积小、制作简单、光谱平坦、谱宽可控的特性，可在超短脉冲产生、生物相干成像和谱分割光源等领域有潜在应用。

关键词：宽谱激光器；非对称量子阱；晶闸管